

Saturated and efficient blue phosphorescent organic light emitting devices with Lambertian angular emission

C. L. Mulder

Department of Electrical Engineering and Computer Science, Massachusetts Institute of Technology, Cambridge, Massachusetts 02139

K. Celebi

Department of Physics, Massachusetts Institute of Technology, Cambridge, Massachusetts 02139

K. M. Milaninia

Department of Materials Science and Engineering, Massachusetts Institute of Technology, Cambridge, Massachusetts 02139

M. A. Baldo^{a)}

Department of Electrical Engineering and Computer Science, Massachusetts Institute of Technology, Cambridge, Massachusetts 02139

(Received 22 March 2007; accepted 24 April 2007; published online 22 May 2007)

The authors employ a microcavity to optimize the color of a phosphorescent organic light emitting device (OLED) based on the-sky blue phosphor FIrpic. The output of the OLED is filtered by scattering media to correct the angular emission intensity profile and eliminate the angular dependence of the color. With a holographic diffuser as the scattering medium, the microcavity OLED achieves an external quantum efficiency of $(5.5 \pm 0.6)\%$, as compared to $(3.8 \pm 0.4)\%$ for a conventional structure. The color coordinates of the microcavity OLED with holographic diffuser are $(x, y) = (0.116 \pm 0.004, 0.136 \pm 0.010)$ with minimal angular color shift and a nearly ideal Lambertian angular emission profile. © 2007 American Institute of Physics.

[DOI: [10.1063/1.2742577](https://doi.org/10.1063/1.2742577)]

The development of a stable, efficient, and saturated blue remains an important goal for phosphorescent organic light emitting devices (OLEDs). Unfortunately, it is not sufficient for the energy of the triplet exciton to reach the blue portion of the spectrum, since blue phosphorescence from the triplet exciton is typically diluted by longer wavelength transitions to vibrational excitations of the ground state. For example, the photoluminescent (PL) spectrum of the greenish-blue or “sky-blue” phosphors is not saturated enough for most display applications despite a triplet energy of approximately 2.7 eV.¹ Synthesizing new phosphors with larger triplet energies may not help. Further increases in the exciton energy render a blue phosphor incompatible with most host materials,² limit the molecular design possibilities, and inevitably exacerbate degradation process. Rather, it may be preferable to modify the OLED structure and filter out the unwanted long wavelength phosphorescence. This approach exploits the compatibility of sky blue phosphors with a broader range of host materials and operational lifetimes exceeding 15 000 h at an initial brightness of 200 cd/m².³

The color of a dye can be modified by inserting it within a microcavity.^{4,5} Indeed, a microcavity is formed within a conventional OLED by weak reflections from interfaces. However, the effects of a weak microcavity on the electroluminescence (EL) are relatively minor.⁶ In a strong microcavity, the dye is positioned between two highly reflective films. A strong microcavity significantly modifies the photonic mode density within the OLED, suppressing EL at undesirable wavelengths, and enhancing EL from the homogeneously broadened phosphor at the microcavity resonance.

In this work, we demonstrate an efficient and saturated blue phosphorescent OLED using a strong microcavity. The usual disadvantages of a strong microcavity, namely, the introduction of an angular dependence to the OLED’s color, and a non-Lambertian angular emission profile, are overcome by scattering the emitted radiation.⁷

Strong and weak microcavity OLED structures are compared in Fig. 1(a). The sky-blue phosphor is FIrpic.^{1,8} The strong microcavity is formed by an aluminum cathode and a semitransparent silver anode with a doped⁹ hole transport layer to aid hole injection. The weak microcavity OLED employs the conventional anode of indium tin oxide (ITO) and poly(3,4-ethylenedioxythiophene):poly(4-styrenesulphonate) rather than silver.

The strong microcavity was designed using analytical calculations of the Poynting vector.¹⁰ This technique allows the exact determination of the spectral dependence of energy dissipation in each layer within an OLED [see Fig. 1(b)].¹⁰ To optimize the color of the strong microcavity OLED, the resonant wavelength is blueshifted by approximately 20 nm relative to the peak of the intrinsic PL spectrum of FIrpic at $\lambda = 470$ nm. At the microcavity resonance, the outcoupling fraction is calculated to be nearly 40%. The energy dissipation within the weak microcavity is also shown for comparison. Its outcoupling fraction to air is calculated to be $\sim 30\%$ and only weakly dependent on wavelength.¹⁰ At the resonance, the strong microcavity enhances the photonic mode density for photons emitted in the forward hemisphere at the expense of the waveguide modes that dominate in a weak microcavity OLED.⁵ The calculation also shows that most of the remaining energy in the strong microcavity is dissipated in the semitransparent silver layer, suggesting that replacing

^{a)}Electronic mail: baldo@mit.edu

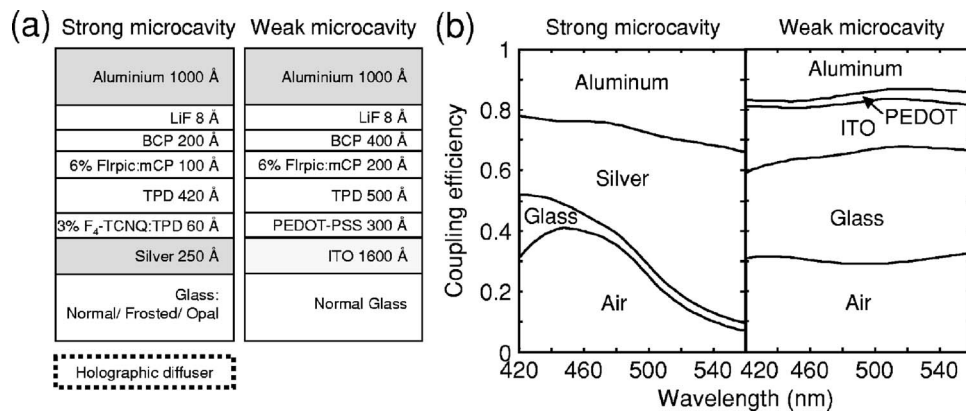


FIG. 1. (a) Structure of the strong microcavity OLED compared to that of a conventional or weak microcavity OLED. In the strong microcavity the anode is a thin, semitransparent layer of Ag. The Al/LiF cathode is defined by a 1 mm diameter shadow mask. The electron transport layer is 2,9-dimethyl-4,7-diphenyl-1,10-phenanthroline (bathocuproine or BCP). To aid hole injection from the silver anode, the first 60 Å of the hole transport layer *N,N'*-diphenyl-*N,N'*-bis(3-methylphenyl)-[1,1'-biphenyl]-4,4'-diamine (TPD) is doped with 3% by mass of the acceptor tetrafluorotetracyanoquinodimethane. The emissive layer consists of 6% by mass iridium(III)bis[(4,6-difluorophenyl)-pyridinato-*N,C'*]picolate (Flrpic) in *N,N'*-dicarbazolyl-3,5-benzene (mCP). The devices were grown directly on the smooth back surface of frosted glass and opal glass diffusers. The holographic diffuser was employed external to devices grown on regular glass. The weak microcavity OLED has an anode precoated with indium tin oxide (ITO) and poly(3,4-ethylenedioxythiophene):poly(4-styrenesulfonate) (PEDOT:PSS). All other layers were deposited by thermal evaporation at a base pressure of less than 3×10^{-6} Torr. Each layer is subject to 20% uncertainty in the interferometric measure of thickness. (b) The calculated distribution of energy dissipation within the OLEDs. In the strong microcavity OLED, energy lost to the cathode, anode, and waveguide modes is labeled, aluminum, silver, and glass, respectively. The remaining energy is outcoupled to air. The modeled layers are Ag 250 Å/TPD 650 Å/mCP 135 Å/BCP 270 Å/Al 1000 Å. In the conventional, or weak microcavity OLED, some energy is dissipated in the aluminum cathode, but most energy is lost to waveguided modes. Roughly 20% of the energy is coupled to waveguide modes in the organic films. These modes are absorbed by the PEDOT and ITO layers. Another ~30% is waveguided within the glass substrate. The modeled layers are ITO 1600 Å/PEDOT:PSS 200 Å/TPD 500 Å/mCP 200 Å/BCP 400 Å/Al 1000 Å.

the silver with a dielectric mirror might further enhance the efficiency.⁵

The measured quantum efficiency of each OLED is shown in Fig. 2(a). Collecting all photons emitted in the forward hemisphere, the peak efficiency for the strong microcavity is $(5.5 \pm 0.6)\%$. The efficiency of the weak microcavity OLED is $(3.8 \pm 0.4)\%$, smaller than the strong microcavity result but consistent with the expected modification in the fraction of radiation outcoupled to air.

Although the strong microcavity enhances the efficiency, optical transmission losses in the scattering filters can be an important source of loss [see Fig. 2(b)]. Three scattering materials were investigated: frosted glass, opal glass, and holographic diffusers.¹¹ Frosted glass is formed by sandblasting the surface of glass. As shown below, it is the weakest scattering medium and it has only moderate optical transmission. Opal diffusing glass consists of an approximately 0.5-mm-thick white flashed opal film supported on glass. It strongly scatters incident light, but its optical transmission is only ~35%. Finally, we characterized holographic diffusers, which are formed by laser patterning of the surface of transparent polycarbonate. The holographic diffuser is ideal for

this application; it is a strong scattering medium with an optical transparency of close to 100%.

The EL spectra as a function of angle from the surface normal are shown in Figs. 3(a) and 3(b), for the strong microcavity OLED without and with the holographic diffuser, respectively. In Fig. 3(a) we compare the EL spectra of the strong microcavity OLED to the intrinsic PL spectrum of Flrpic. The strong microcavity is observed to strongly suppress the undesirable long wavelength emission, but there is a noticeable color shift with angle. Higher wave numbers are enhanced for large emission angles, yielding a blueshift in the EL spectrum that is constrained only by the sharp high energy shoulder of the Flrpic PL spectrum. With the holographic diffuser, however, the color shift is barely perceptible and compares well to the expected EL spectrum after transmission through an ideal scattering medium. This prediction is obtained from the intrinsic PL spectrum of Flrpic and the calculated strong microcavity outcoupling spectrum from Fig. 1(b). The color coordinates for all devices are shown in Fig. 3(c). The average color coordinates are deep blue $(x, y) = (0.116 \pm 0.004, 0.136 \pm 0.010)$, significantly

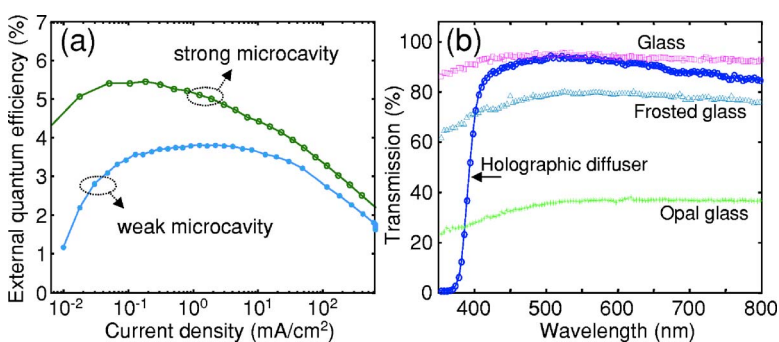


FIG. 2. (Color online) (a) External quantum efficiency of the strong microcavity Flrpic OLED compared to the performance of a conventional weak microcavity device built on ITO/PEDOT:PSS rather than silver. The comparison demonstrates that the strong microcavity increases the efficiency of the OLED. All devices were measured in a nitrogen environment to minimize degradation. (b) The optical transmission efficiencies of our glass substrates compared to the three diffusing filters, frosted glass, opal glass, and the holographic diffuser. Of the scattering filters, the holographic diffuser exhibits the highest optical transparency.

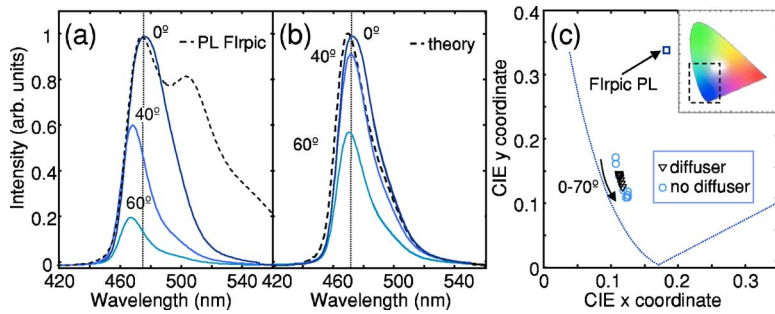


FIG. 3. (Color online) Electroluminescent spectra of the strong microcavity FIrpic OLED as a function of angle from the surface normal (a) without and (b) with the holographic diffuser. A solid angle cone of 0.6° was collected at each rotational position. With the holographic diffuser the color shift is barely perceptible. For comparison in (a) we plot the intrinsic photoluminescent spectrum of FIrpic and in (b) we plot the modeled electroluminescent spectrum of the strong microcavity after transmission through an ideal scattering filter. (c) The color coordinates of the strong microcavity devices with holographic diffusers are deep blue with $(x,y) = (0.116 \pm 0.004, 0.136 \pm 0.010)$. The intrinsic FIrpic photoluminescence spectrum is sky blue with $(x,y) = (0.18, 0.34)$. Inset: the full CIE diagram identifying the expanded blue region.

shifted from the intrinsic PL spectrum of FIrpic: $(x,y) = (0.18, 0.34)$.

In Fig. 4, we plot the angular profile of EL from the strong microcavity OLEDs. In the absence of scattering, the intensity is maximized normal to the OLED stack, yielding a non-Lambertian emission profile, and potentially causing a large angle-dependent color shift if strong microcavity OLEDs are employed in display applications with conventional green and red Lambertian OLEDs. The addition of a frosted glass filter barely alters the angular profile. The opal and holographic diffusers, however, are observed to yield near ideal Lambertian profiles, rendering these devices suitable for display applications.

Surface and cross sectional scanning electron micrographs of the holographic diffuser are shown in Figs. 4(b) and 4(c), respectively. The scattering film is approximately $10 \mu\text{m}$ thick and lateral surface features are on the order of

$5 \mu\text{m}$. Provided that the scattering film is placed within $\sim 100 \mu\text{m}$ of the OLED's semitransparent electrode, a diffuser with similar or smaller feature sizes is appropriate in high definition displays.

To summarize, we have coupled strong microcavity OLEDs with scattering filters. The scattering filter corrects the angular dependence of EL, and the strong microcavity gives a deep blue color with enhanced optical outcoupling. The demonstrated benefits to color and efficiency suggest that this architecture—strong microcavity OLEDs combined with a scattering filter—can be generally implemented to the benefit of red, green, and blue pixels in three color display applications. We also note that the maximum reported external quantum efficiency of a sky-blue phosphor is nearly triple that of the control device reported here,³ suggesting that stable, saturated blue OLEDs with external quantum efficiencies exceeding 10% are within reach.

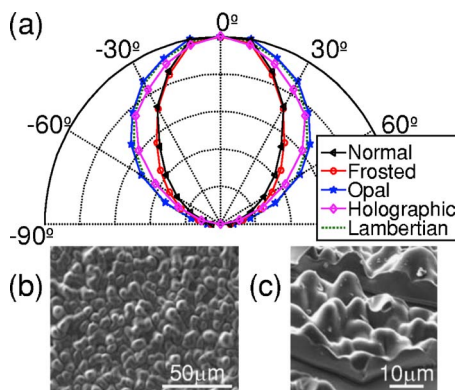


FIG. 4. (Color online) (a) Angular emission profile of the strong microcavity FIrpic OLED as a function of angle from the surface normal, together with its modification by the three diffusing filters. Opal glass and the holographic diffuser both yield nearly ideal Lambertian emission patterns, but the holographic diffuser has superior optical transparency. A solid angle cone of $\sim 4^\circ$ was collected at each rotational position. [(b) and (c)] Scanning electron micrographs of the surface and cross section, respectively, of the holographic diffuser.

¹C. Adachi, R. C. Kwong, P. Djurovich, V. Adamovich, M. A. Baldo, M. E. Thompson, and S. R. Forrest, *Appl. Phys. Lett.* **79**, 2082 (2001).

²R. J. Holmes, B. W. D'Andrade, S. R. Forrest, X. Ren, J. Li, and M. E. Thompson, *Appl. Phys. Lett.* **83**, 3818 (2003).

³M. S. Weaver, R. C. Kwong, V. A. Adamovich, M. Hack, and J. J. Brown, *J. Soc. Inf. Disp.* **14**, 449 (2006).

⁴T. Tsutsui, N. Takada, S. Saito, and E. Ogino, *Appl. Phys. Lett.* **65**, 1868 (1994).

⁵R. H. Jordan, L. J. Rothberg, A. Dodabalapur, and R. E. Slusher, *Appl. Phys. Lett.* **69**, 1997 (1996).

⁶V. Bulovic, V. B. Khalfin, G. Gu, P. E. Burrows, D. Z. Garbuzov, and S. R. Forrest, *Phys. Rev. B* **58**, 3730 (1998).

⁷Y.-S. Tyan, J. D. Shore, G. Farruggia, and T. R. Cushman, *SID Int. Symp. Digest Tech. Papers* **2005**, 142 (2005).

⁸R. J. Holmes, S. R. Forrest, Y.-J. Tung, R. C. Kwong, J. J. Brown, S. Garon, and M. E. Thompson, *Appl. Phys. Lett.* **82**, 2422 (2003); FIrpic and mCP were obtained from Luminescence Technology Corp. 2F, No. 21 R&D Road, Science-Based Industrial Park, Hsin-Chu, Taiwan, R.O.C. 30076.

⁹W. Y. Gao and A. Kahn, *J. Appl. Phys.* **94**, 359 (2003).

¹⁰K. Celebi, T. D. Heidel, and M. A. Baldo, *Opt. Express* **15**, 1762 (2007).

¹¹Edmund Optics, 101 East Gloucester Pike, Barrington, NJ 08007-1380. The holographic diffusers had a scattering angle profile of 80° .